EPJ Web of Conferences **318**, 02001 (2025) https://doi.org/10.1051/epjconf/202531802001
AAPM-III 2025

Geomagnetic data real-time forecast based on neural networks

Yurii Polozov*

Institute of Cosmophysical Research and Radio Wave Propagation FEB RAS, Mirnaya st., 7, Paratunka, Kamchatskiy krai, 684034, Russian Federation

Abstract. Earth magnetosphere has a complex structure and its state is estimated by geomagnetic indexes. The paper suggests an approach to make real-time forecast of SME geomagnetic index variations. The approach is based on the combination of neural networks and wavelets. The features of input data formation for neural network models and forecast results are shown. The obtained neural network models can be applied in geomagnetic state monitoring problems.

1 Introduction

Earth magnetic field state affects the operation of technical equipment in many fields. Among them are the systems for information transfer, operation of high and space crafts, ground energy infrastructure. The specific examples may be geo-induced current (GIC) occurrences in long-distance networks, which reach 200-300 A [1, 2] and make significant impact on health and safety.

Magnetospheric processes have a complex structure [3] and form different current systems. The disturbances there are mainly initiated by the Sun. To estimate the magnetic field intensities, magnetic indexes, reflecting the magnetosphere state, are considered. One of the important parameters of the magnetic field are the changes of the auroral current, which is often estimated on the basis of AE [4] or SME [5] indexes. The SME index, obtained in the SuperMAG project, reflects the dynamics of the auroral current even during its shift from polar latitudes.

Timely estimate of the SME index state makes it possible to obtain the information on the volume of the energy penetrating into geospheric shells. The relation between auroral currents and space weather parameters was illustrated, for example, in the paper [6]. Thus, forecast of the SME index is an acute problem. The paper, based on early investigations [7], presents the approach for constructing the model of magnetic index variations. In order to solve this problem, wavelets and long short-term memory (LSTM) neural networks are used. Neural networks (NN) allow us to construct models of complex nonstationary data [8, 9], which are the SME index time series. The existing limitations in application of NN, associated with input data quality [8], are solved in that paper by wavelet processing. Wavelets make it possible to represent initial data in the form of a component set [10] that provides separation of data structures, falling on neural networks, into different vectors.

* Corresponding author: up_agent@mail.ru

However, when applying wavelets to realize data real-time processing, the problem of boundary effect is to be solved. This problem causes sudden change of wavelet coefficients at the time series boundary that complicates neural network model performance.

The paper presents complex approach to the real-time forecast of the SME index data based on neural networks of LSTM architecture. The approach is based on the formation of input vectors taking into account the specific character of NN training and decrease of boundary effect impact when using wavelets. The suggested approach allowed us to realize the SME index forecast in real time.

2 Methodology

2.1 Problem statement

The SME index has a complicated structure depending on interplanetary magnetic field (IMF) effect. IMF vertical component Bz impact on the Earth magnetosphere results in geomagnetic storm development [11, 12]. Construction of a neural network model for the SME index and its forecast are possible, when using retrospective data of the SME and IMF Bz data [7]. The paper combines the NNs with wavelet decomposition to forecast geomagnetic field state using the data of IMF Bz and SME index. Neural network model provides high quality of SME approximation [7] for several counts ahead. However, it is difficult to apply it in real time due to the boundary effect, when using wavelets [10, 13]. Figure 1 shows an example of wavelet coefficient changes during SME index decomposition into the scale levels 1, 10 and 19. Arrows indicate the effect range on wavelet coefficient values when data supply is stopped (Figure 1(c)), that is typical for real-time forecast. Depending on the scale level and, subsequently, the wavelet length, the changes in the coefficients may last for tens of hours. This affects the trained neural network system performance, when making real-time forecast of the SME index.

It is possible to solve this problem when two approaches are simultaneously used, they are: decrease of boundary effect impact and formation of a training set for the NN with the boundary effect.

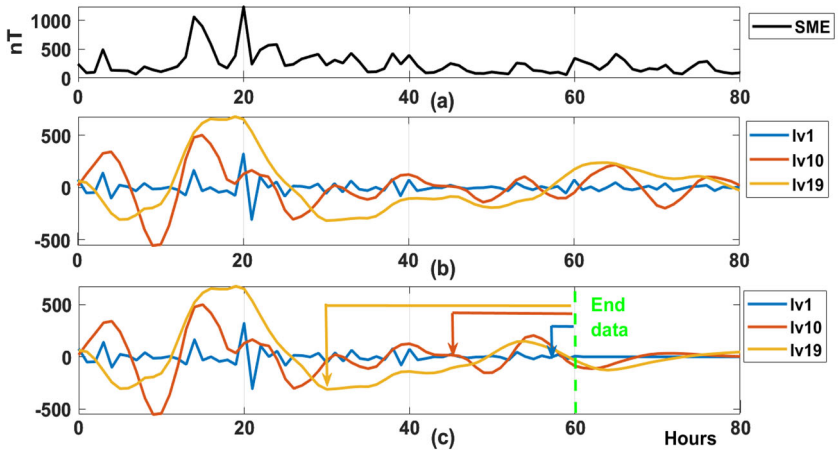

Fig. 1. (a) – SME index data; (b) – wavelet decomposition coefficients of the initial SME index; (c) – wavelet decomposition coefficients when SME index data supply is stopped (vertical dashed line).

2.2 Applied data

The NNs were trained and tested on IMF BZ and SME data with the sampling of 1 hour. Data for 1999-2022 were used. The IMF state was recorded on the Advanced Composition Explorer space craft (GSM coordinates), the project electronic address is https://omniweb.gsfc.nasa.gov. The SME index time series were provided by the SuperMAG project, the electronic address https://supermag.jhuapl.edu.

2.3 Data representation in the form of wavelet coefficient intensity

It was shown in the paper [7] that the dynamics of changes in IMF Bz and geomagnetic indexes can be represented in the form of intensity by wavelets. This representation is based on the scale decomposition of data [11]:

$$\left(W_\Psi s_{y,x}\right) := |x|^{-\frac{1}{2}} \int_{-\infty}^{+\infty} s(t)\Psi\left(\frac{t-y}{x}\right) dt,\ s \in L^2(R),\ x,\ y \in R,\ x \neq 0, \quad (1)$$

where Ψ is the basic wavelet, x is the scale, y is the time. The wavelet coefficients obtained on the basis of (1) are estimated the sign as

$$W_\Psi s_{y,x} = \begin{cases} (W_\Psi s_{y,x})^+ \ , if\ W_\Psi s_{y,x} > 0 \\ (W_\Psi s_{y,x})^- \ , if\ W_\Psi s_{y,x} \leq 0 \end{cases}. \quad (2)$$

After coefficient decomposition, we determine their intensities on different ranges of the scale D:

$$T_y^{\pm} = \sum_D (W_\Psi s_{y,x})^{\pm}. \quad (3)$$

2.4 Presentation of data for NN training

The LSTM-architecture neural networks are the developments of recurrent networks and can be applied in the modeling of complex data sets, having inner dependencies expanded in time (counts) [14]. In a general case, the LSTM network is formed on the basis of memory blocks organizing connected sub-networks. The LSTM networks are described in detail, for example, in [15]. The NN architecture, used in the paper, consisted of 14 input vectors, 256 neurons of a hidden layer. Its quality was estimated on the basis of a root-mean-square error (RMSE) and a mean absolute percentage error (MAPE).

$$RMSE = \sqrt{\frac{1}{N}\sum_{i=1}^{N}(z_i - \hat{z}_i)^2},$$

$$MAPE = 100\%\frac{1}{N}\sum_{i=1}^{N}\left|\frac{z_i - \hat{z}_i}{z}\right|,$$

where N is the sampling length, z_i are the SME data, $\hat{z}_i$ is the NN forecast.

General representation of the LSTM network is illustrated in Figure 2.

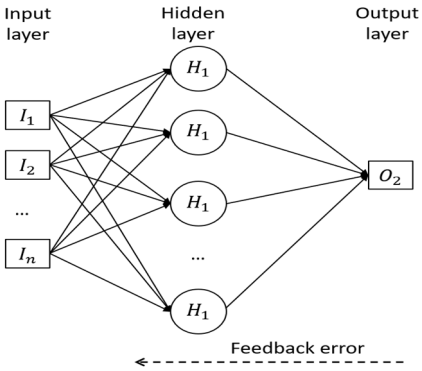

Fig. 2. Architecture of the LSTM model.

The training data for the NN were formed on the basis of 14 input vectors, including the SME and IMF Bz data and their wavelet-coefficient intensities distributed into the ranges D (2), (3). The distribution into the ranges was based on the results of the paper [7]. This allowed us to divide the data into frequency periods affecting the SME dynamics. The SME and IMF Bz initial data were divided into segments with the duration of 72 hours on the basis of a moving time window. Each segment was added at its ends by 48 counts to compensate the boundary effect. The procedure of the count adding is described below. Then, wavelet processing was carried out on the basis of (2) and (3). The data, added for the boundary effect compensation, were removed, and 2-D matrices of input vectors were formed to be supplied to the NN input. The general dimension of each matrix was 12x72 values. The scheme for input data formation is illustrated on the example of the SME index in Figure 3.

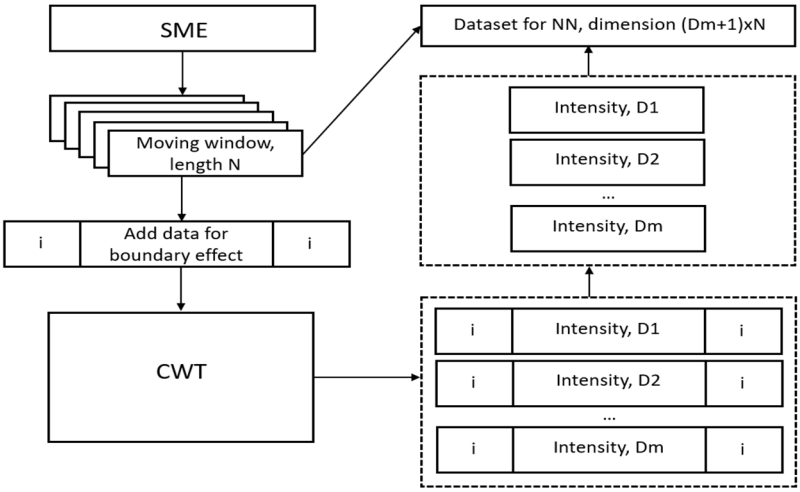

Fig. 3. Scheme of input data formation for the NN.

3 Experiment results

A common way to compensate the boundary effect on wavelet coefficients is the data adding at time series ends. This paper solves the problem of the SME index forecast, thus, values for the preceding hours are added before a time series processed by wavelets (Figure 3). This allows us to avoid the boundary effect in the left (initial) part of a time series. It is impossible to add data into the right part due to their absence in real-time forecast. In order to decrease the boundary effect in the right part, three ways of data adding were applied, they are: ME, MI, MID.

$$ME_k = \frac{1}{p}\sum_{k-p}^{k-1} z_i,$$

where p is the number of counts used to for the current count.

MI and MID are the initial time series mirrored with respect to the end. The difference between MI and MID is that the mirrored segment in MI is $N-1, N-2, \dots, N-l$, and MID is represented as $N, N-1, N-2, \dots, N-l-1$, were N is the final count of the initial time series.

Estimates of NNs performance efficiency for different ways of filling the mirrored segment is shown in Table 1. The NNs were trained on prepared data sets with different ways of the mirrored segments and tested on the data not used during the training.

Table 1. Estimates of NN performance efficiency for mirrored data adding.

	ME	**MI**	**MID**
RMSE	126	120	129
MAPE	72	70	88

Table 1 illustrates that the way of construction of a mirrored segment relatively the latest count of a time series (MI) has the highest efficiency.

Figure 4 shows the results of NN performance for the period March 2, 2012 – March 14, 2012, when making the real-time forecast of the SME data. Two magnetic storms occurred during the indicated period (with the commencement on March 7 and 8). They affected the SME index dynamics. The Figure shows the complicated structure of the SME time series, which had been disturbed from March 2. Sudden increases in the value amplitudes after the magnetic storms commencements coincide with the NN forecast data (indicated by arrows). That shows the trained NN performance efficiency in the estimation of the initial period of strong disturbances and the energy volume, which can penetrate into the magnetosphere.

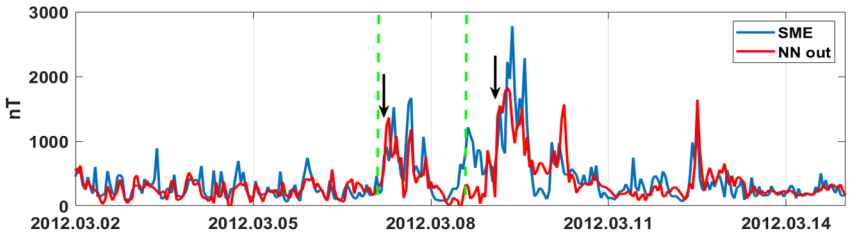

Fig. 4. Results of the real-time forecast of SME index hourly data for the period March 2, 2012 – March 14, 2012. Green dashed line shows the magnetic storms commencements.

4 Conclusion

The approach to the training data formation, suggested in this paper, to forecast the SME index by the LSTM neural networks and wavelets showed the possibility of estimating the magnetic field dynamics in real time. The way of data adding in order to decrease the boundary effect showed the least error when the mirrored segment is constructed relatively the latest count. The obtained neural network system provides the forecast of the SME index variations during disturbances and can be applied in the systems for geomagnetic state monitoring.

The work was supported by IKIR FEB RAS State Task (subject registration No. 124012300245-2).

References

1. V. Pilipenko, Space weather impact on ground-based technological systems. Sol.-Terr. Phys. **7**, 68-104 (2021).
2. R. Pirjola, A. Pulkkinen, A. Viljanen, Adv. Space Res. **31**, 795-805 (2003).

3. N.Yu. Ganushkina, M.W. Liemohn, S. Dubyagin, Reviews of Geophysics **56**, 309-332 (2018).
4. T.N. Davis, M. Sugiura, J. Geophys. Res. **71**, 785-801 (1966).
5. P.T. Newell, J.W. Gjerloev, J. Geophys. Res. **116**, 2011JA016936 (2011).
6. A. Marques De Souza, E. Echer, M.J.A. Bolzan, R. Hajra, Ann. Geophys. **36**, 205-211 (2018).
7. Y. Polozov, *SME Geomagnetic index data forecast based on wavelet transform and LSTM neural networks, in Solar-Terrestrial relations and physics of earthquake precursors* (Springer Nature Switzerland, Cham, 2023), 186-196.
8. S.S. Haykin, *Neural networks: a comprehensive foundation* (Prentice Hall, Upper Saddle River, N.J, 1999).
9. A.D. Smorodinov, T.V. Gavrilenko, V.A. Galkin, Vestnik of KRAUNC. Fiz.-mat. nauki. **2**, 69-86 (2023).
10. S.G. Mallat, *A wavelet tour of signal processing: the sparse way* (Academic Press, Boston, 2009).
11. J.W. Dungey, Phys. Rev. Lett. **6**, 47-48 (1961).
12. R.P. Kane, J. Geophys. Res. **110**, A02213 (2005).
13. J.M. Lilly, Proc. R. Soc. A. **473**, 20160776 (2017).
14. S. Hochreiter, J. Schmidhuber, Neural Computation. **9**, 1735-1780 (1997).
15. G. Van Houdt, C. Mosquera, G. Nápoles. Artif Intell Rev. **53**, 5929-5955 (2020).